

Electric Field Induced Gelation of Poly(3-Thiopheneacetic Acid)/Polydimethylsiloxane Fluids

Datchanee Chotpattananont¹, Anuvat Sirivat^{*1} and Alexander M. Jamieson²

¹Conductive and Electroactive Polymers Research Unit, The Petroleum and Petrochemical College, Chulalongkorn University, Bangkok 10330, Thailand

²Department of Macromolecular Science, Case Western Reserve University, Cleveland, OH 44106-7202, USA

Abstract: Electrorheological (ER) properties under oscillatory shear of perchloric acid doped-poly(3-thiopheneacetic acid)/oil (P3TAA/silicone) suspensions have been investigated. The effects of electric field strength, silicone oil viscosity, and particle concentration were investigated. When the electric field strength reaches a critical value, the P3TAA-based ER fluid exhibits transitional behavior between the sol and gel states, at which point the equilibrium rheological properties satisfy the Winter-Chambon transition criteria. The critical electric field strength required for the sol-gel transition to occur, as determined by a frequency-independent loss tangent, decreases with increasing particle concentration. The effect of oil viscosity on the ER behavior has its greatest effect at weak electric field strength. Based on the sol-gel transition criteria, the viscoelastic scaling exponent n is found to vary between 0.83-0.98, with increasing particle concentration, corresponding to fractal dimension values between 1.61 and 1.06, respectively. The critical gel strength parameter decreases with increasing particle concentration, which correlates to the decreasing critical electric field strength.

Keywords: Gelation, electrorheological fluid, conductive polymer, poly(3-thiopheneacetic acid).

INTRODUCTION

Electrorheological (ER) fluids are typically composed of electrically polarizable particles dispersed in a low-dielectric oil. It is generally well known and accepted that the ER effect is the result of particle agglomeration, forming fibrillar strings oriented along the electric field direction. In the absence of an electric field, ER fluids typically show Newtonian viscometric behavior. Upon application of an electric field, the particles become polarized, creating field-induced dipoles, which attract one another, and cause the particles to form chains or fibrillar structures between two electrodes along the direction of electric field. These chains are held together by interparticle forces which have sufficient strength to inhibit fluid flow [1]. The connectivity between the particles in the strings arises from the field-induced dipoles. The agglomeration of the particles inevitably affects the viscoelastic behavior of ER fluids, resulting in an increase of the shear viscosity. In particular, if the developing structure possesses sufficient rigidity, the ER fluid is expected to exhibit a liquid-solid transition or a sol-gel transition.

Gelation occurs when aggregation or cross-linking of molecules or particles takes place chemically or physically within a liquid matrix. As a result, the system undergoes a transformation from a solution or dispersion state to an elastic solid called a gel, which consists of a sample-spanning network of molecules or particles permeated by the liquid matrix [2]. Rheological properties are primary and sensitive

tools to investigate the onset of such network formation, because at the gel point, network connectivity occurs, and flow is inhibited.

Winter and Chambon [3, 4] first elucidated the rheological conditions that define the point at which an aggregating system transforms from a sol to a gel. Considering oscillatory shear experiments, in the sol state, the storage and loss moduli exhibit typical predominantly viscous behavior at low frequencies, i.e. $G''(\omega) > G'(\omega)$ and frequency dependence determined by the relaxation time spectrum of molecular or particle clusters:

$$G'(\omega) = A\omega^{n'} \quad \text{and} \quad G''(\omega) = B\omega^{n''} \quad (1)$$

with $n' = 2.0$ and $n'' = 1.0$. At the sol-gel transition point, a sample-spanning critical network cluster is first formed, and a different frequency dependence is predicted, with $n' = n'' = n$, originating in a self-similar structure of the critical gel cluster [3,4]:

$$G'(\omega) = A\omega^n \quad \text{and} \quad G''(\omega) = B\omega^n \quad (2)$$

and

$$\tan \delta = G''/G' = B/A = \tan(n\pi/2) \quad (3)$$

The storage and the loss moduli share the same frequency scaling exponent value, n , and $\tan \delta$ become independent of frequency. As aggregation continues, the elasticity increases and ultimately, $G'(\omega)$ becomes frequency independent and larger than $G''(\omega)$. At the gel point, defined by Eqs. (2)-(3), a characteristic materials parameter, S , the gel strength of the critical network cluster can be determined as [3, 4]:

$$S = G' \omega^{-n} \Gamma(1-n)^{-1} \cos(n\pi/2) \quad (4)$$

$$S = (A^2 + B^2)^{1/2} \Gamma(n) \sin(n\pi/2) \quad (5)$$

*Address correspondence to this author at the Conductive and Electroactive Polymers Research Unit, The Petroleum and Petrochemical College, Chulalongkorn University, Bangkok 10330, Thailand; Tel: +662 218 4131; Fax: +662 611 7221; E-mail: anuvat.s@chula.ac.th

where $\Gamma(n)$ is the gamma function.

A wide variety of systems exhibit a sol-gel transition having rheological behavior consistent with the above predictions, ranging from those that form networks *via* covalent cross-linking [3-5] to diverse systems that form networks *via* non-covalent interactions, including proteins [6], polysaccharides [7], polymer-surfactant complexes [8], and colloids [9].

The question as to whether ER fluids exhibit a rheological sol-gel transition in concordance with the predictions of Eqs. (1)-(3) was first addressed by Chin and Winter [10]. Their study utilized a model ER fluid consisting of monodisperse silica spheres (diameter $1.0 \pm 0.1 \mu\text{m}$), dispersed in a polydimethylsiloxane oil (viscosity 0.5 Pa.s). It was demonstrated that, with increase of field strength, the rheology changes from Newtonian liquid to viscoelastic liquid to viscoelastic solid (gel). The gel point, as defined by Eqs. (1)-(4) occurred at a relatively low field strength, before the appearance of sample-spanning particle strings in the optical microscope, and could be observed only for relatively low particle concentrations. Thus the actual gel point appears to be determined by the formation of particle clusters near the walls and in the bulk fluid, not visible in the optical microscope. The appearance of sample-spanning strings occurs at higher field strength, and seems to correlate closely to the crossover point, where $G'(\omega)$ becomes larger than $G''(\omega)$ at low frequencies, and where a finite yield stress appears [10].

Particles based on conducting polymers are an attractive vehicle to form ER fluids, due to their high intrinsic polarizability [11]. These particles are often highly irregular in shape, and highly polydisperse in size. It is of interest to investigate whether a sol-gel transition point can be identified for such systems *via* rheological measurements. A first study, which sought to answer this question, was performed [12] on a suspension of polyaniline (PANI) in silicone oil and failed to identify such a sol-gel transition. The failure was tentatively ascribed to the wide polydispersity of the PANI particles. However, a solid-liquid transition indicated by a $G'-G''$ crossover was observed, and its characteristics studied as a function of particle concentration and silicone oil viscosity [13].

In this work, we investigate the equilibrium rheological properties of an ER system consisting of a particulate dispersion of the conductive polymer, poly(3-thiopheneacetic acid) (P3TAA) in silicone oil, under an applied electric field. It will be shown that, provided the silicone oil viscosity is sufficiently high, when the electric field strength reaches a critical value, the equilibrium rheological properties indeed satisfy the sol-gel transition condition, where $\tan \delta$ becomes independent of frequency [3, 4]. The effect of P3TAA particle concentration on the frequency scaling exponent, n , and the gel strength parameter, S , will be reported here.

EXPERIMENTAL

Materials and ER Fluids Preparation

3-thiopheneacetic acid, 3TAA (AR grade, Fluka) was used as the monomer. Anhydrous ferric chloride, FeCl_3 (AR grade, Riedel-de Haen) was used as the oxidant. Chloroform, CHCl_3 (AR grade, Lab-Scan) and methanol, CH_3OH (AR grade, Lab-Scan) were dried over CaH_2 for 24 hours under the nitrogen atmosphere and then distilled. Perchloric acid

dopant, HClO_4 (AR grade, AnalaR) was used as received. Two silicone oils were used as the dispersing phase (AR grade, Dow Corning) with density 0.96 g/cm^3 and kinematic viscosities of 100 and 500 cSt; each was vacuum-dried and stored in a desiccator prior to use.

As in our previous work [12, 14], we used particles of poly(3-thiopheneacetic acid), PTAA, which were synthesized *via* oxidative polymerization [15]. The synthesized PTAA particles were treated with perchloric acid in order to obtain a highly controlled level of conductivity [16]. All the PTAA particles used in this study have essentially the same electrical conductivity, broad size distribution, and highly irregular shapes [12, 14].

The electrorheological, ER, fluids were prepared by dispersing HClO_4 doped PTAA particles in the silicone oils and then placed within an ultrasonicator for 30 minutes at $25 \pm 0.1 \text{ }^\circ\text{C}$. The prepared ER fluids were then stored in a desiccator prior to use and redispersed again prior to each measurement.

Oscillatory Shear Experiments

A fluid rheometer (Rheometrics, ARES) was used to measure various rheological properties. It is fitted with a custom-built copper parallel-plates fixture (diameter of 50 mm) attached to insulating plexiglass sheets. A DC voltage was applied with either a DC power supply (Tektronic, PS280) or a custom-built DC power supply, which can deliver an electric field strength up to 2 kV/mm. A digital multimeter (Tektronic, CDM250) was used to monitor the voltage and current. To ensure formation of an equilibrium agglomerate structure, the electric field was applied for 10 minutes before measurements were taken. Each measurement were carried out at a temperature of $25 \pm 0.1 \text{ }^\circ\text{C}$ and repeated at least two or three times.

In our experiments, storage G' and loss G'' moduli were measured as functions of frequency and electric field strength. Strain sweep tests were first carried out to determine the strains appropriate for both G' and G'' to fall in the linear viscoelastic regime. The appropriate strain was determined to be 0.1% for the electric field strengths of 2, 1, 0.5 kV/mm, 1% for the electric field strengths of 200, 100, 80 V/mm, and 10% for the electric field strengths of 50, 20, 10, 1, 0 V/mm. The deformation frequency was varied from 0.01 to 100 rad/s.

RESULTS

The mean P3TAA particle diameter was determined to be approximately $30 \mu\text{m}$ with a standard deviation of $\sim 8 \mu\text{m}$. SEM monographs indicated the shapes of the undoped and doped P3TAA particles were highly irregular [13]. The particle concentration and silicone oil viscosity of the HClO_4 doped P3TAA suspensions are listed in Table 1.

The effect of particle concentration on the equilibrium electrorheological properties of the suspensions was investigated. Particle concentrations investigated were 5%, 10%, and 20% by weight (corresponding to volume fractions of 0.024, 0.048, and 0.092, respectively) at a specific electrical conductivity of $7.5 \times 10^{-2} \text{ S/cm}$ (HPT5, HPT10, and HPT20).

Fig. (1) shows the dynamic mechanical properties of a 20 wt% suspension of highly doped P3TAA in 0.1 Pa.s silicone oil (HPT20/ η 0.1). The results show that the dynamic moduli,

$G'(\omega)$ and $G''(\omega)$, of the P3TAA suspensions increase dramatically by nearly 8-9 orders of magnitude as the electric field strength is increased through the range of 0-2 kV/mm. In the absence of an electric field, the suspension is fluid and exhibits liquid-like behavior in which G'' is significantly larger than G' over the entire range of frequency.

Table 1. Particle Concentration and Silicone Oil Viscosity of HClO₄ Doped PTAA Suspensions

System	Particle Concentration (% wt.)	Viscosity of Silicone Oil (Pa.s)
HPT5/ η 0.1	5	0.1
HPT10/ η 0.1	10	0.1
HPT20/ η 0.1	20	0.1
HPT5/ η 0.5	5	0.5
HPT10/ η 0.5	10	0.5
HPT20/ η 0.5	20	0.5

Evidently, as seen by the least squares fits in Fig. (1), G' and G'' deviate from the expected frequency dependence (Eq. (1)) in the absence of the electric field (exponents n' and $n'' = 0.7$ and 0.9 , respectively, instead of 2.0 and 1.0). Departure from the ideal ω^2 behavior of G' was observed by Chin and Winter [10] at high concentrations in their silica/silicone oil ER fluid (30 wt%). They attributed this to elasticity produced by particle agglomerates formed *via* a weak water-bridging effect and van der Waals interaction between the silica particles. Another factor was the lack of rheometer sensitivity to reach lower frequencies, where the ω^2 relation is expected [10]. In our experiments, when the fraction of P3TAA particles was reduced to lower concentrations of 10 wt% (HPT10/ η 0.1) and 5 wt% (HPT5/ η 0.1), we found similar behavior of G' and G'' , except that the dynamic moduli were smaller. A strong deviation of G' from the ideal ω^2 behavior was still observed even at low particle concentrations.

The effect of silicone oil viscosity on the ER response of the suspensions was investigated. Fig. (2) shows the dynamic

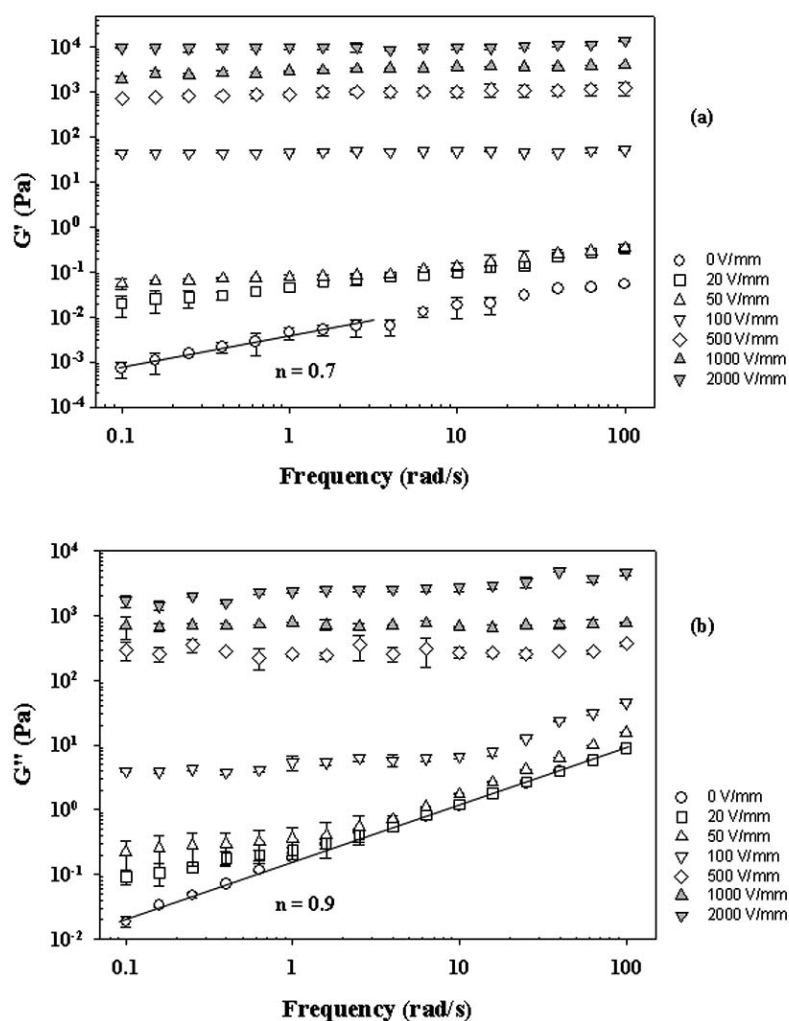


Fig. (1). Storage and loss moduli vs frequency of 20% wt. HClO₄-doped polythiophene/0.1 Pa.s silicone oil suspension (HPT20/ η 0.1) at 25 \pm 0.1 $^{\circ}$ C: (a) the storage modulus G' ; and (b) the loss modulus G'' .

mechanical properties of 20 wt% of highly doped P3TAA in 0.5 Pa.s silicone oil (HPT20/ η 0.5). Again, the dynamic moduli, $G'(\omega)$ and $G''(\omega)$, of the HPT20/ η 0.5 suspensions increase dramatically by about 8 orders of magnitude, as the electric field strength is increased through the range of 0-2 kV/mm. However, now we find that, at zero field, the suspension exhibits more ideal fluid-like behavior; i.e., the frequency exponents are more closely in agreement with Eq. 1 (n' and $n'' = 1.7$ and 1.0, c.f. 2.0 and 1.0, respectively). Noting that, for monodisperse systems at sufficiently low frequencies, $G' \sim \omega^2 \tau^2$ and $G'' \sim \omega \tau$, where τ is a characteristic molecular weight-dependent relaxation time, this may indicate a decreased role of particle polydispersity when the matrix viscosity is increased, and the elastic response of the ER fluid becomes less dominant [17].

The effect of oil viscosity on the dynamic mechanical properties can be clearly observed by comparing Figs. (1) and (2). At low to moderate electric fields (0-100 V/mm), G' shows a significant decrease in the system with the higher oil viscosity. However, at higher fields, G' is comparable in both systems or slightly higher in the system with lower vis-

cosity. In contrast to G' , the loss modulus G'' increases with oil viscosity at all field strengths, reflecting an increased viscous response from the fluid. These results are in agreement with observations of Sakurai *et al.* [17], who interpret the dependence of ER response on matrix viscosity in terms of a model based on a competition between the dipole-dipole electrostatic interaction (which acts to promote association of neighboring particles) and the shearing force due to the viscous flow of the matrix (which acts to separate the particles). In the polarization model, the application of an electric field polarizes the particles, creating induced dipole moments, which lead to an electrostatic interaction between particles:

$$F_{elec} = \frac{3\pi p^2}{8\epsilon_s r^4} \quad (6)$$

where ϵ_s is the dielectric constant of matrix, r is the distance between particles, and $p = (\pi/2)\epsilon_s a^3 [(\sigma_p - \sigma_s)/(\sigma_p + 2\sigma_s)]E_0$, where a is radius of particle, E_0 is the electric field strength, and σ_p , σ_s are the electrical conductivities of the particle and matrix, respectively. On the other hand, the hydrodynamic

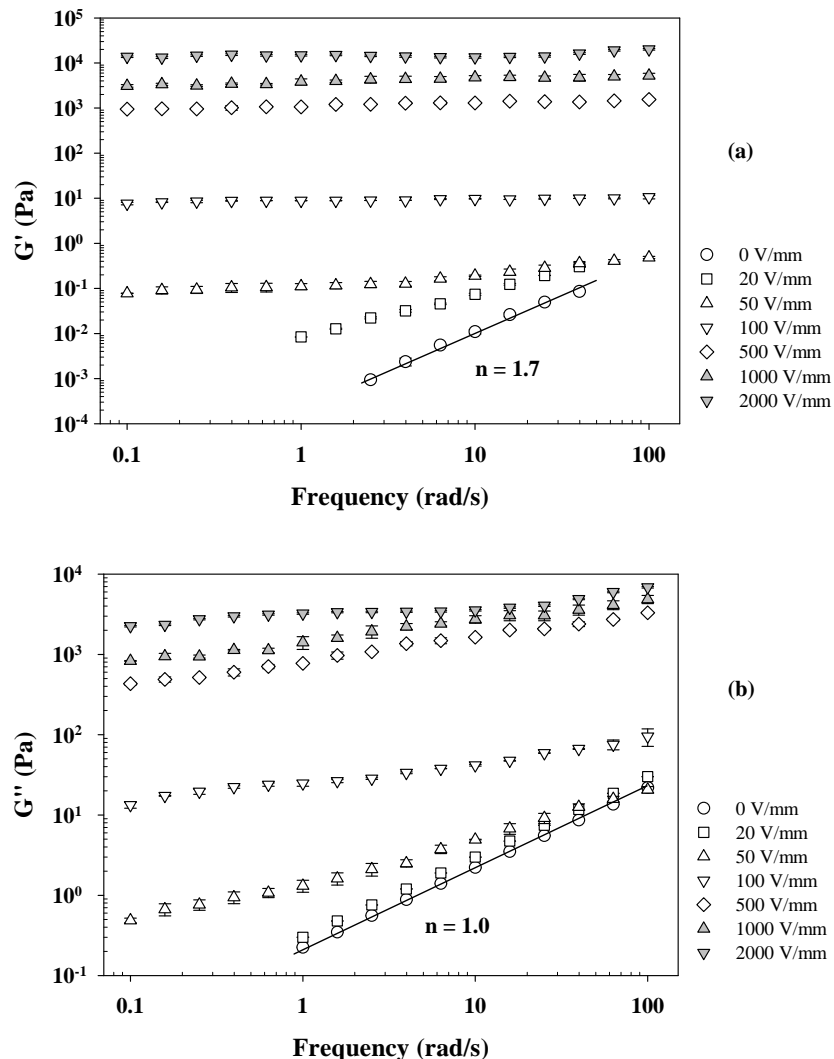


Fig. (2). Storage and loss moduli vs frequency of 20% wt. HClO₄-doped polythiophene/0.5 Pa.s silicone oil suspension (HPT20/ η 0.5) at 25 \pm 0.1 $^{\circ}$ C: (a) the storage modulus G' ; and (b) the loss modulus G'' .

force, which is generated from the difference between the velocity of the particle, v_p , and the ambient solvent velocity, v_s , can be written as

$$F_{\text{shear}} = 6\pi\eta a(v_s - v_p) \quad (7)$$

where η is the solvent viscosity.

If the electric field is weak and the viscosity is large so that F_{shear} dominates over F_{elec} , the storage modulus G' is expected to decrease as the viscosity is further increased since the relatively weak electrostatic interactions will be less able to form aggregates of larger size. On the other hand, if the electric field is strong, F_{elec} will dominate the particle interactions, and larger particle aggregates will form leading to increased flow resistance and thus increased G' .

From Figs. (1) and (2), it also clearly seen that, with increase of field strength, the responses of G' and G'' pass through the typical features of a liquid-to-solid transition. Thus, at low field strengths, $G'' \gg G'$ ($\tan \delta \gg 1$). With in-

crease in field strength, the storage modulus undergoes a particularly large increase, whereas the loss modulus lags behind, and hence a $G'-G''$ crossover occurs, so that, at high field strengths, G' and G'' each become essentially frequency independent with $G' \gg G''$ ($\tan \delta \ll 1.0$). The liquid-to-solid transition occurs because of formation of fibrillar structures by the P3TAA particles in the presence of the electric field, as reported previously [13].

The question arises whether the rheological data of the P3TAA ER fluid shows a sol-gel transition point as described by the theory embodied in Eqs. (2) – (4). To answer this, in Fig. (3a), we replot the data of Fig. (1) for the 20 wt% suspension of highly doped P3TAA in 0.1 Pa.s silicone oil (HPT20/ η 0.1) in the form of the loss tangent, $\tan \delta = G''(\omega)/G'(\omega)$, vs frequency. We see that the slope of $\tan \delta$ is distinctly positive at electric field strengths $E \leq 50$ V/mm, and becomes smaller than unity at higher electric field strength. Thus, a definitive condition where $\tan \delta$ is zero

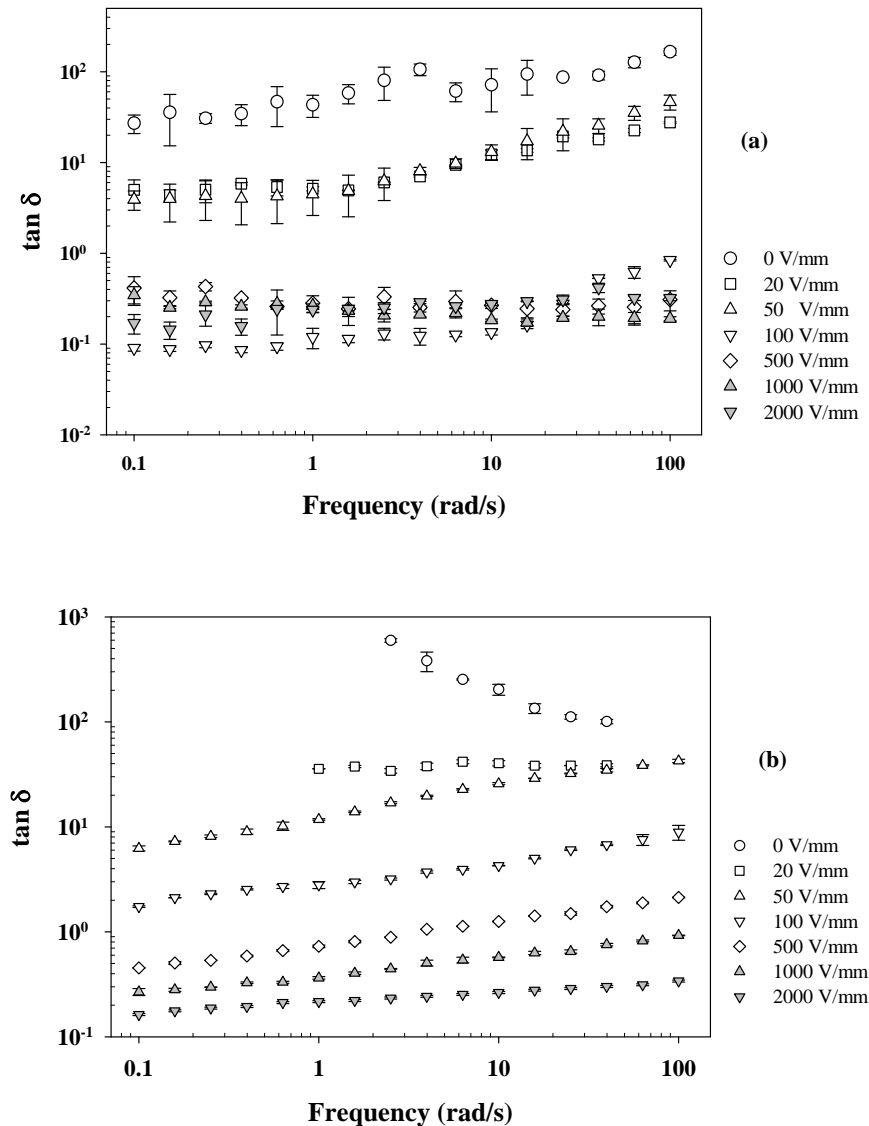


Fig. (3). Plots of $\tan \delta$ vs frequency of HClO₄ doped polythiophene/silicone oil suspensions as various electric field strengths: (a) HPT20/ η 0.1; and (b) HPT20/ η 0.5.

cannot be ascertained. Chin and Winter observed similar behavior in their highest particle concentration system [9], i.e. that the slope of $\tan \delta$ was already positive in the absence of the field. They suggested that possible formation of water-bridges between the particles may cause sufficient connectivity for the suspension to show early solid-like behavior. Likewise, in our low viscosity silicone system, P3TAA particles may have formed agglomerations in the absence of electric field, which contribute to the anomalous value of the frequency scaling exponent $n' = 0.7$ of G' in Fig. (1a). An additional factor is that the precision of the $\tan \delta$ values are relatively low because of the low viscosity. We note parenthetically that a few gelling systems which do not obey the Winter-Chambon criterion have been reported [18-20], indicative that these systems do not have a self-similar structure of the critical gel.

Plots of $\tan \delta$ vs frequency at various electric field strengths for the 20 wt% suspension of highly doped P3TAA in 0.5 Pa.s silicone oil (HPT20/ η 0.5) are presented in Fig. (3b). Here a distinct change in slope of $\tan \delta$ from negative to positive with increasing electric field strength is evident, and a condition where $\tan \delta$ is frequency independent can be observed at a field strength of 20 V/mm, characteristic of the sol-gel transition point, according to the Winter-Chambon criterion [3, 4]. Evidently, the higher viscous response at low frequencies, which also contributes to a more ideal behavior of the frequency scaling exponents, leads to a definitive manifestation of a critical sol-gel transition in this ER fluid system. These observations demonstrate for the first time to our knowledge that a sol-gel transition that follows the Winter-Chambon criteria can occur in an ER fluid consisting of polydisperse polarizable particles with irregular shapes.

The effect of particle concentration on this sol-gel transition has been further investigated, by suspending the P3TAA particles in 0.5 Pa.s silicone oil at different concentrations: 5%, 10%, and 20% by weight (HPT5/ η 0.5, HPT10/ η 0.5, and HPT20/ η 0.5, respectively). A similar general behavior pattern was observed for all systems. Thus we do not show the results of those systems but summarize their properties in Table 2. For HPT10/ η 0.5, the slope of $\tan \delta$ becomes frequency independent at a higher electric field strength of about 40 V/mm, and, for the HPT5/ η 0.5 system the corresponding condition occurs at a still higher electric field strength, i.e. 50 V/mm.

The experimentally obtained frequency scaling exponents, n' and n'' , and coefficients A and B, obtained by fits of $G'(\omega)$ and $G''(\omega)$ to Eq. (1), for our polythiophene suspensions are shown in Table 2. From Table 2, the power law exponent n' decreases and approaches 0 as electric field strength is increased while n'' also decreases, but approaches a small finite value ≈ 0.1 . The values of n' and n'' approximately coincide at a critical field strength which is identified as the gelation point, according to the Winter-Chambon criteria. The resulting values of the critical gel exponent n in our systems, deduced from the values of $\tan \delta$ *via* Eq. (3), increase from 0.83 to 0.98, as particle concentration increases, and the critical electric field strength decreases from 50 V/cm to 20 V/cm.

Finally we note that, in agreement with Chin and Winter [10], as the field strength increases beyond the sol-gel transition point, a $G'-G''$ crossover occurs. Such a crossover is observed even for the lower viscosity ER fluids, which do not show a Winter-Chambon sol-gel transition. This is illustrated for the HPT20/ η 0.1 suspension, in Fig. (4), which

Table 2. Winter-Chambon Scaling Parameters of HClO₄ Doped PTAA Suspensions in Silicone Oils at Temperature of 25 °C

System	E (V/mm)	n'	n''	n_{avg}	d_f	A, B (y-Intercepts)	S (Pa s ⁿ) (eq.10)
HPT5/ η 0.5	0	1.95	0.99	1.47	-	1.8×10^{-4} , 0.14	-
	20	1.87	0.98	1.42	-	3.2×10^{-3} , 0.18	-
	50	0.84	0.82	0.83	1.54	0.03, 1.08	0.03
	100	0.13	0.55	0.34	-	1.04, 6.9	-
	500	0.08	0.42	0.25	-	602.6, 138.1	-
	1000	0.09	0.31	0.20	-	1718.2, 791.8	-
	2000	0.04	0.11	0.08	-	7506.6, 1984.8	-
HPT10/ η 0.5	0	1.83	0.99	1.41	-	2.2×10^{-4} , 0.16	-
	20	1.52	0.99	1.26	-	5.8×10^{-3} , 0.21	-
	40	0.92	0.92	0.92	1.39	0.02, 0.94	0.02
	50	0.84	0.84	0.84	-	0.06, 1.17	-
	100	0.17	0.55	0.36	-	1.4, 10.7	-
	500	0.06	0.42	0.24	-	978.7, 672.2	-
	1000	0.08	0.31	0.20	-	3246.5, 1108.3	-
2000	0.05	0.11	0.08	-	8701.6, 2611.3	-	
HPT20/ η 0.5	0	1.72	0.99	1.36	-	2.4×10^{-4} , 0.2	-
	20	0.98	0.99	0.98	1.28	8.3×10^{-3}, 0.3	8.1×10^{-3}
	50	0.12	0.43	0.28	-	0.1, 1.4	-
	100	0.04	0.25	0.14	-	8.7, 25.1	-
	500	0.07	0.30	0.18	-	1096.5, 831.8	-
	1000	0.08	0.26	0.17	-	3801.9, 1445.4	-
	2000	0.01	0.09	0.05	-	14454.4, 3020.0	-

plots G' and G'' at a frequency of 0.1 rad/s vs electric field strength. The suspension exhibits a crossover where $G'(0.1)$ becomes larger than $G''(0.1)$ at a field strength of 60 V/mm. The dependence of this transition point on system variables was extensively explored for an ER fluid based on polyaniline by Hiamtup *et al.* [13].

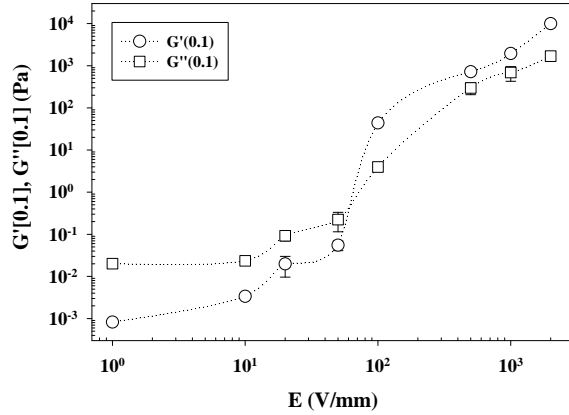


Fig. (4). Electric field dependence of the storage and loss moduli of 20% wt. HClO_4 highly doped polythiophene/0.1 Pa.s silicone oil suspension (HPT20/ η 0.1) at $25 \pm 0.1^\circ\text{C}$, measured at a frequency of 0.1 rad/s.

DISCUSSION

The values of the critical scaling exponent, n , from Eq. 4 and Eq. 5, obtained for our P3TAA ER fluid fall in the range 0.83-0.98. As observed by Chin and Winter [10], the power-law scaling of the critical gel occurs at very low field strengths, persists over a relatively limited frequency range, of the order two decades, and is typically truncated at the low frequency end by the limited sensitivity of the rheometer. Chin and Winter [10] do not quote values for their critical exponents, but, approximately, from their data, since at the gel point, $\tan \delta \sim 30 - 40$, they appear to be comparable to our values, i.e. of the order of $n = 1.0$. As noted by Chin and Winter [10], power-law frequency dependence of G' and G'' is expected over a frequency range that probes the internal relaxation modes on length scales where the system has a self-similar structure.

Various theoretical treatments [21-25] have attempted to predict values of the critical frequency scaling exponents, for comparison with the literature data, which encompass a wide range of values within the allowed range $0 < n < 1$. Thus, for an end-linked poly(dimethylsiloxane) values of n between 0.19 and 0.92 were obtained, depending on stoichiometry, concentration and molecular weight [5]. Likewise, for inorganic systems, values ranging from 0.13 [26] to 0.75 [27] have been observed. Thus the values obtained for ER fluids fall at the upper limit of allowable values, based on the Winter-Chambon criteria for gelation.

Generally, theories which describe power-law behavior at the gel point relate the power-law exponent to the relaxation spectrum of a critical gel cluster with a self-similar structure. Thus, the scaling exponent, n , can generally be related to the mass fractal dimension, d_f , characterizing the relationship between the radius of gyration of the particular self-similar

structure and its molar mass; $R_g^{d_f} \sim M$. According to Muthukumar [26], for semi-dilute, unentangled solutions of monodisperse polymers, having a fractal dimension d_f , and fully-screened hydrodynamic interactions (Rouse dynamics), theoretical analysis leads to

$$n = \frac{\bar{d}_f}{(\bar{d}_f + 2)} \quad (8)$$

where \bar{d}_f is the fractal dimension of the polymer when the excluded volume effect is fully screened [25]:

$$\bar{d}_f = \frac{2d_f}{(d + 2 - 2d_f)} \quad (9)$$

For a polydisperse solution of fractal polymers,

$$n = \frac{d_f(\tau - 1)}{d_f + 2} \quad (10)$$

where τ is a scaling exponent that describes the size polydispersity near the gel point. Interestingly, from Eq. (10), adopting the classical Zimm-Stockmayer model of gelation ($d_f = 4$, $\tau = 5/2$), we have $n = 1.0$. Alternatively [25], adopting the percolation theory and assuming the hyperscaling relation

$$\tau = 1 + d/d_f \quad (11)$$

where d is the dimensionality of space, Eq. (10) leads to:

$$n = d/(d_f + 2) \quad (12)$$

From Eq. (12), with $d = 3$, it follows that n changes from 1 to 0.6 for a fractal structure in the physically-realizable domain $1 \leq d_f \leq 3$. If the excluded volume is screened out, then the corresponding expression for n is [25]:

$$n = d/(\bar{d}_f + 2) \quad (13)$$

Substituting Eq. (8) in Eq. (12), we have [25]:

$$n = \frac{d(d + 2 - 2d_f)}{2(d + 2 - d_f)} \quad (14)$$

Now all values of the scaling exponent $0 < n < 1$ become possible for fractal values in the physically-realizable domain $1 \leq d_f \leq 3$. In addition, Muthukumar points out [25] that, if there is only partial screening of the excluded volume, then the fractal dimension to be specified in Eq. (13) will be some value that lies between d_f and \bar{d}_f . Thus, it appears, a viscoelastic scaling exponent, n , having a value comparable to unity can be explained *via* Eq. (10), assuming fractal polymers with excluded volume and screened hydrodynamic interactions, which follow classical gelation theory ($d_f = 4$). Considering the fibrillar nature of the agglomerates in ER fluids, this seems an inappropriate model. Turning instead to the percolation model, Eq. (14), which assumes full screening of excluded volume and hydrodynamic interactions, and, inserting the values of $n = 0.83, 0.92$, and 0.98 , we arrive at $d_f = 1.54, 1.39$, and 1.28 . If we instead consider Eq. (12), i.e the percolation model with Rouse dynamics and unscreened excluded volume interaction, inserting $n = 0.83$,

0.92, and 0.98, we arrive at $d_f = 1.61, 1.26, \text{ and } 1.06$. Intuitively, considering the structures formed are predominantly fibrillar, the last set of results seems most reasonable, i.e. as the volume fraction increases, and the critical field strength decreases, the fractal dimension tends towards a value of unity i.e. a straight line.

Finally, recalling Eq. (5), we can determine the strength, S , of the critical gel network. The values of A and B can be obtained from the intercepts of fits to Eq. (1) of log-log plots of G' and G'' versus frequency. Taking the HPT20/ η 0.5 suspension at a field strength of 20 V/mm for example, the values of A and B , obtained from the intercept at $\log \omega = 0$, yield an S value of about $8.1 \times 10^{-3} \text{ Pa s}^n$. In Table 2, we summarize the results for the power law exponents n' , n'' , as well as the average n , and the S parameter for the experiments in which the sol-gel transition conditions (Eqs. 4 and 5) are satisfied. Evidently, from Table 1, the S values decrease with increase in particle concentration. The electrostatic polarization model [28, 29] predicts that the stress in an ER fluid scales as the particle volume fraction times the square of the electric field. If we assume S follows this scaling, then it is predicted that S would decrease by a smaller factor, $\times 0.6$, compared to the observed $\times 0.26$. However, as noted above, at the low fields where the sol-gel transition occurs, the opposing viscous force also plays an important role. Assuming from Eq. (8), that this scales as volume fraction times oil viscosity, it follows that S should then simply scale as the square of the critical field. This predicts a larger decrease of $\times 0.16$ compared with the observed $\times 0.26$. Thus, reality seems to be a situation intermediate between these two extremes. In any event, qualitatively, the observed decrease in S with increasing volume fraction coupled to a lower critical field strength appears to be consistent with the theoretical expectation that the decrease in polarization stress dominates over the increased contribution from the viscous stress. Physically, higher volume fraction means that more particles are available to become incorporated into thicker, more numerous fibrillar agglomerates at the gel point, whereas a lower field strength induces a lower dipole moment and decreases the strength of the interparticle interactions resulting in thinner, less numerous, and less rigid fibrillar agglomerates.

CONCLUSIONS

In this study, we have investigated the equilibrium rheological properties of suspensions of a conductive polymer, polythiophene, under the influence of electric field. Our results show that the PTAA suspension exhibits viscoelastic behavior and a transition from fluid-like to solid-like behavior as the electric field strength is increased. In agreement with the idea that the viscoelastic response of the ER fluid is determined by a balance between the driving polarization force and the opposing viscous force, increased oil viscosity significantly enhances the viscous response (G'') relative to the elastic response (G') at low to moderate electric field (0-100 V/mm), but has less effect at high field strengths. Furthermore, it was observed that the equilibrium rheological properties of our PTAA suspensions in the higher viscosity silicone oil exhibit a sol-gel transition as defined by the Winter-Chambon criterion, in which $\tan \delta$ becomes independent of frequency, when a sufficiently strong electric field strength is applied. The critical electric field strength for the

transition is found to decrease with increasing particle concentration. Moreover, the values of the power law exponent, n , increase through the range 0.83-0.98, as the particle concentration increases from 5 wt % to 20 wt%. Correspondingly, the fractal dimension of the critical gel cluster increases toward a value of unity, characteristic of linear structures. Finally, the gel strength parameter S decreases as the particle concentration increases, which appears to be determined by the fact that the critical field strength, and hence the associated polarization stress, each decrease with increased concentration. Our results show that such a transition occurs for ER fluids consisting of polydisperse particles with highly irregular shapes, as well as in model systems based on monodisperse spheres.

ACKNOWLEDGEMENTS

The authors would like to acknowledge the financial supports provided by the Thailand Research Fund, TRF-RGJ grant no. PHD/0128/2542 and TRF-BRG the Conductive and Electroactive Polymers Research Unit of Chulalongkorn University, the Centre of Excellence for Petroleum Petrochemicals and Advanced Materials, and the Royal Thai Government (Budget of Fiscal Year 2551). AMJ wishes to acknowledge the financial support of the National Science Foundation, Polymers Program, through award DMR0513010.

REFERENCES

- [1] Bonnecaze, R.T.; Brady, J.F. Dynamic simulation of an electrorheological fluid. *J. Chem. Phys.*, **1992**, *96*, 2183-2202.
- [2] Stauffer, D.; Coniglio, A.; Adam, M. Gelation and critical phenomena. *Adv. Polym. Sci.*, **1982**, *44*, 103-158.
- [3] Winter, H.H.; Chambon, F. J. Analysis of linear viscoelasticity of a crosslinking polymer at the gel point. *J. Rheol.*, **1986**, *30*, 367-382.
- [4] Chambon, F.; Winter, H.H. Elasticity and failure in composite gels. *J. Rheol.*, **1987**, *31*, 683-697.
- [5] Scanlan, J. C.; Winter, H. H. Composition dependence of the viscoelasticity of end-linked poly(dimethylsiloxane) at the gel point. *Macromolecules*, **1991**, *24*, 47-54.
- [6] Hsu, S.H.; Jamieson, A.M. Viscoelastic behaviour at the thermal sol-gel transition of gelatin. *Polymer*, **1992**, *34*, 2602-2608.
- [7] Rwei, S.P.; Chen, I.Y.; Cheng, Y.Y. Sol/gel transition of chitosan solutions. *J. Biomat. Sci. Polym. Ed.* **2005**, *16*, 1433-1445.
- [8] Nyström, B.; Kjoniksen, A.L.; Lindman, B. Effects of temperature, surfactant, and salt on the rheological behavior in semidilute aqueous systems of nonionic cellulose ether. *Langmuir*, **1996**, *12*, 3233-3240.
- [9] Shay, J.S.; Raghavan, S.R.; Khan, S.A. Thermoreversible gelation in aqueous dispersions of colloidal particles bearing grafted poly(ethylene oxide) chains. *J. Rheol.*, **2001**, *45*, 913-927.
- [10] Chin, B.D.; Winter, H.H. Field-induced gelation, yield stress, and fragility of an electro-rheological suspension. *Rheol. Acta.*, **2002**, *41*, 265-275.
- [11] Cho, M.S.; Kim, J.W.; Choi, H.J.; Jhon, M.S. Polyaniline and its modification for electroresponsive material under applied electric fields. *Polym. Adv. Tech.*, **2005**, *16*, 352-356.
- [12] Chotpattananont, D.; Sirivat, A.; Jamieson, A.M. Electrorheological properties of perchloric acid-doped polythiophene suspensions. *Colloid Polym. Sci.*, **2004**, *282*, 357-365.
- [13] Hiamtup, P.; Sirivat, A.; Jamieson, A.M. Electrorheological properties of polyaniline suspensions: Field-induced liquid to solid transition and residual gel structure. *J. Colloid Interface Sci.*, **2006**, *295*, 270-278.
- [14] Chotpattananont, D.; Sirivat, A.; Jamieson, A.M. Scaling of yield stress of polythiophene suspensions under electric field. *Macromol. Mater. Eng.*, **2004**, *289*, 434-441.
- [15] Kim, B.; Chen, L.; Gong, J.; Osada, Y. Titration behavior and spectral transitions of water-soluble polythiophene carboxylic acids. *Macromolecules*, **1999**, *32*, 3964-3969.

- [16] Chen, L.; Kim, B.; Nishino, M.; Gong, J.; Osada, Y. Environmental responses of polythiophene hydrogels. *Macromolecules*, **2000**, *33*, 1232-1236.
- [17] Sakurai, R.; See, H.; Saito, T.; Sumita, M. Effect of matrix viscoelasticity on the electrorheological properties of particle suspensions. *J. Non-Newtonian Fluid Mech.*, **1999**, *81*, 235-250.
- [18] Chiou, B.; Raghavan, S.R.; Khan, S.A. Effect of colloidal fillers on the cross-linking of a UV-curable polymer: gel point rheology and the Winter-Chambon criterion. *Macromolecules*, **2001**, *34*, 4526-4533.
- [19] Ilvasky, M.; Bubenikova, Z.; Bouchal, K.; Nedbal, J. Solubility and dynamic mechanical behaviour of polyurethane systems at the critical molar ratio of the reactive groups for gelation and at the gel point. *Polymer*, **1996**, *37*, 3851-3860.
- [20] Seetapan, N.; Mai-ngam, K.; Plucktaveesak, N.; Sirivat, A. Linear viscoelasticity of thermoassociative chitosan-g-poly(N -isopropylacrylamide) copolymer. *Rheol. Acta.*, **2006**, *45*, 1011-1018.
- [21] Martin, J.E.; Adolf, D.; Wilcoxon, J.P. Viscoelasticity of near-critical gels. *Phys. Rev. Lett.*, **1988**, *61*, 2620.
- [22] Durand, D.; Delsanti, M.; Adam, M.; Luck, J.M. Frequency dependence of viscoelastic properties of branched polymers near gelation threshold. *Eur. Phys. Lett.*, **1987**, *3*, 297-301.
- [23] Rubinstein, M.; Colby, R.H.; Gillmor, J.R. Scaling properties of branched polyesters. 2. Static scaling above the gel point. *J. Am. Chem. Soc.*, **1989**, *30*, 81-82.
- [24] Muthukumar, M. Dynamics of polymeric fractals. *J. Chem. Phys.*, **1985**, *83*, 3161-3168.
- [25] Muthukumar, M. Screening effect on viscoelasticity near the gel point. *Macromolecules*, **1989**, *22*, 4656-4658.
- [26] Ponton, A.; Barboux-Doueff, S.; Sanchez, C. Rheology of titanium oxide based gels: determination of gelation time versus temperature. *Colloids Surf. A*, **2000**, *162*, 177-192.
- [27] In, M.; Prud'homme, R.K. Fourier transform mechanical spectroscopy of the sol-gel transition in zirconium alkoxide ceramic gels. *Rheol. Acta*, **1993**, *32*, 566-565.
- [28] Klingenberg, D.J.; Swol, F.V.; Zukoshi, C.F. The small shear rate response of electrorheological suspensions. I. Simulation in the point-dipole limit. *J. Chem. Phys.*, **1991**, *94*, 6160- 6169.
- [29] Klingenberg, D.J.; Swol, F.V.; Zukoshi, C.F. The small shear rate response of electrorheological suspensions. II. Extension beyond the point-dipole limit. *J. Chem. Phys.*, **1991**, *94*, 6170-6178.

Received: September 8, 2008

Revised: October 22, 2008

Accepted: October 29, 2008

© Chotpattananont *et al.*; Licensee Bentham Open.

This is an open access article licensed under the terms of the Creative Commons Attribution Non-Commercial License (<http://creativecommons.org/licenses/by-nc/3.0/>) which permits unrestricted, non-commercial use, distribution and reproduction in any medium, provided the work is properly cited.